RESEARCH ARTICLE

Stand-alone power-to-X production dynamics

A multi-method approach to quantify the emission-cost reduction trade-off

Uwe Langenmayr ⓘ | **Paul Heinzmann** | **Alexander Schneider** | **Manuel Ruppert** |
Andreas Rudi | **Wolf Fichtner**

Institute for Industrial Production (IIP),
Karlsruhe Institute of Technology (KIT),
Karlsruhe, Germany

Correspondence
Uwe Langenmayr, Institute for Industrial
Production (IIP), Karlsruhe Institute of
Technology (KIT), Karlsruhe, Germany.
Email: uwe.langenmayr@kit.edu

Editor Managing Review: Luk Van Wassenhove

Abstract

Power-to-X (PtX) processes allow for increased utilization of renewable energy in sectors like transportation, heat, and industry, where greenhouse gas emissions are hard to abate or irreducible. However, due to significantly higher production costs than conventional alternatives and the requirement of lower greenhouse gas footprints, PtX processes must aim for low-cost and low-emission production. This work introduces a multi-method approach by combining process simulation, techno-economic analysis, life cycle assessment, renewable electricity generation modeling, and multi-objective optimization to investigate the relationship between PtX production costs and greenhouse gas emissions to support investment decisions. The approach is applied to produce renewable hydrogen, Fischer–Tropsch crude, and methanol by considering global weather data with hourly temporal resolution. Our results show that locations with high wind capacity factors achieve the lowest costs and greenhouse gas emissions, and locations with high solar PV capacity factors perform worst in the context of greenhouse gas emissions when producing PtX products, primarily due to the emission-intensive production of solar PV modules. Locations with mixed capacity factors of wind and solar PV allow cost-efficient greenhouse gas emissions reduction since solar PV capacities can be substituted with a combination of wind generation capacities and battery storage. In addition, flexible PtX technologies reduce costs and greenhouse gas emissions significantly since fewer auxiliary components, like storage, are needed.

KEYWORDS
industrial ecology, multi-method approach, multi-objective optimization, open source, power-to-X, renewable energy carriers

1 | INTRODUCTION AND LITERATURE REVIEW

The transformation of the electricity sector is in full swing toward renewable energies. Other sectors, such as industry, heating, agriculture, and transportation, need to increase their share of renewable energy to defossilize. While electrification of processes provides suitable, cost-effective,

and efficient solutions for many processes, not all processes can be electrified. Especially if the energy carriers are used as feedstock, for example, in ammonia production, electrification is not an alternative (International Energy Agency [IEA], 2021, 2023).

Offering an option of indirect electrification, power-to-X (PtX) processes help to increase the share of renewable energy beyond the supply of renewable electricity by transforming electrical energy into chemical energy (Oyewo et al., 2024). Stand-alone PtX facilities are of particular interest, since favorable locations regarding land availability and capacity factors of the renewable generators, without the limitation of grid availability, can be chosen to produce large quantities of PtX products at low costs. Not relying on grid electricity avoids additional costs like taxes and levies, and avoids grid electricity with a potential high share of conventional energy carriers, which is necessary to comply with the European regulation of grid electricity supply to produce renewable electricity-based PtX products (European Union, 2023).

The coupling element between electric energy and chemical energy carriers in PtX facilities is mainly based on electrolysis processes, with water electrolysis as the most common technology (Rego de Vasconcelos & Lavoie, 2019). In combination with renewable electricity, power-to-gas (PtG) technologies produce green hydrogen. Hydrogen can be used directly or as an intermediate product, transported, or stored in a gaseous or liquid state. A potential large-scale off-taker of green hydrogen might be the steel industry, where the direct reduction of iron ore offers a future low-carbon alternative to blast furnace ovens (Jacobasch et al., 2021). Other PtG applications include the production of gaseous fuels and energy carriers based on hydrogen, like synthetic natural gas (SNG) (Götz et al., 2016; Tremel, 2018).

In power-to-liquid applications, green hydrogen is used as an intermediate to generate liquid fuels and energy carriers, like synthetic methanol (MeOH) or Fischer–Tropsch (FT) synthesis-based sustainable aviation fuels (SAF) (Schmidt et al., 2018; Schorn et al., 2021). Power-to-liquid and advanced PtG applications rely on the supply of additional input streams besides green hydrogen. Carbon sources, mainly CO_2, are needed to generate synthetic hydrocarbons (SNG, SAF, e-Diesel, and MeOH), while renewable ammonia production relies on nitrogen supply (Tremel, 2018). FT synthesis-based hydrocarbons offer a broad range of applications where fuels with high energy densities are needed, such as aviation, sea shipping, and chemical industries (De Klerk, 2008; Dry, 1999). MeOH is required primarily in today's chemical industries as a base chemical but can be used as an intermediate for many products in the future by applying processes like methanol-to-olefins, methanol-to-gasoline, or methanol-to-jet, or as a marine fuel (Schemme et al., 2020).

In summary, PtX concepts are as broad as their application areas. Still, even though they enable the increase of renewable energy in manifold sectors, only a few have been commercialized so far since low-cost and renewable production faces manifold challenges (IEA, 2024). PtX technologies require multidisciplinary research to investigate their potential from technological, economic, and environmental dimensions, while the interaction of different technologies also needs to be addressed. Renewable electricity generation (RES-E) volatility and region-specific renewable availability are especially new challenges for operators of conventional synthesis systems, which prevent the application of off-the-shelf solutions.

We have identified and compared studies investigating PtX plants (see Table 2 in Section A1 of Supporting Information S1). The research on PtX plants is characterized by several dimensions that can be assessed using different methodologies, approaches to consider RES-E generation, and objectives. Looking at methods, life cycle assessments (LCA) calculate the life cycle impact of defined systems to investigate criteria, such as the environmental or social impact of the system (Campos-Guzmán et al., 2019; Hoppe et al., 2018; Koj et al., 2019; Werker et al., 2019). Process simulations aim to create realistic models of chemical plants to assess technical feasibility and scalability while improving processes. They are often combined with techno-economic assessments (TEA) to estimate costs and evaluate economic feasibility using spreadsheet calculations (Albrecht et al., 2017; Heinzmann et al., 2021; Runge et al., 2020). TEAs can also be conducted solely based on literature values (Armijo & Philibert, 2020; Morgan et al., 2017) and integrated into optimization approaches like linear programming (LP) or mixed-integer linear programming (Berger et al., 2021; Maggi et al., 2020).

The definition of the system precedes the actual LCA. The same applies to TEAs based on process simulations, where the process simulation defines the system. The consumption of feedstocks is assumed to be steady and often integrated into calculations by applying constants. When studying RES-E generation, such constants are usually the levelized electricity costs and yearly capacity factors (Kadam & Yadav, 2024; Schack et al., 2016). A first approach to address the limitations of such a simplification is to consider RES-E generation in separate models. Osman et al. (2020) model hydrogen supply as an LP. Fasihi et al. (2016) overlay the RES-E generation profiles to calculate the levelized costs of electricity generation and yearly capacity factors. Both works use the results of their RES-E modeling in subsequent, separate models. However, even though the RES-E generation is considered, it is reduced to a single parameter in the main model. More advanced approaches model the RES-E generation with the PtX plant by integrating capacity factor profiles of renewable generators with a resolution of up to 1 h (Berger et al., 2021; Sherwin, 2021). Such approaches consider the volatility and availability of RES-E generation and allow for more realistic decisions.

The above-mentioned literature focuses on single objectives, like calculating production costs or environmental or social life cycle impacts. However, single objectives might ignore potential trade-offs between different objectives. Studies increasingly use multi-criteria assessment to close this research gap. In Lee et al. (2022) and Terlouw et al. (2024), production costs and greenhouse gas (GHG) emissions are considered. However, their approach assesses both objectives independently. Multi-objective optimization (MOO) is applied to consider both objectives simultaneously. For instance, whereas Farajiamiri et al. (2023) use MOO to calculate the trade-off between production costs, land use, and water use, Kenkel et al. (2021) investigate the trade-off between production costs and GHG emissions.

The review of existing literature shows a clear gap in the systematic evaluation of the entire PtX chain. Steady-state methods like LCA, process simulations, and spreadsheet-based TEAs can provide detailed information on the plant. However, the volatility of RES-E generation is reduced to a

constant. In addition, LCA and spreadsheet-based TEAs are only applicable to defined systems and cannot be used to derive optimal facility design regarding environmental or economic objectives. Conversely, approaches with more sophisticated methods of integrating RES-E generation often simplify the technical, economic, and ecological characteristics of PtX plants. Finally, most approaches concentrate on single objectives, ignoring potential inconsistencies and trade-offs of multiple objectives like production costs and GHG emissions. The identified research gap leads to the following research questions:

1. How can a systematic evaluation of the entire PtX plant be implemented?
2. How is the trade-off between production costs and GHG emissions characterized, and how can it provide decision support for PtX plant investments?
3. What are the key decisions to reduce production costs and GHG emissions of PtX products?
4. How do different technologies and locations perform compared to each other, and what are the key drivers of these performances?

Our research aims to overcome the mentioned limitations by systematically developing a holistic methodology to evaluate the entire PtX process chain. First, we use process simulation to gain in-depth information on feedstocks, auxiliary materials, chemical conversions, and plant capacity dimensions. We combine the derived information with TEA and LCA to understand the economic and environmental impact of each process chain's components. Second, we enrich the information with temporally and geographically highly resolved RES-E profiles within a multi-objective mixed-integer linear optimization to investigate each process performance in the context of volatile renewable generation. The combination of TEA, LCA, and optimization allows the calculation of optimal capacities concerning economic and environmental objectives based on the location-specific RES-E generation. With this approach, the limitations of individual methods are addressed and synergies exploited (see Figure 1 in Section A2 of Supporting Information S1). For example, the limitation of LCA regarding the necessary predefinition of the plant design and simplified RES-E consideration can be addressed, and the environmental assessment can be scaled to numerous individual locations. Similar holds for the process simulation methodology in combination with spreadsheet-based TEA. To our knowledge, such a holistic approach has not been conducted yet. This approach allows for decision support in the context of PtX investments by providing detailed insights into developing optimal production costs, greenhouse gas emissions, capacities, and operations at a high temporal and geographical resolution. Based on individual preferences, strategic decisions can be made on optimal locations, capacities, and operations while quantifying production costs and GHG emissions. The developed multi-method approach is showcased using green hydrogen, FT crude, and MeOH production. This manuscript's results and discussion section will focus mainly on the MOO, and the results and discussion of the process simulation, LCA, and TEA will be presented in Sections A3.3, A3.5, and A4.3 of Supporting Information S1.

2 | METHODOLOGY

The following chapter describes the developed method of this work, which is further depicted in the graphical abstract in Figure 1. While we apply the complete methodology to fully understand the underlying technology and derive technical, economic, and environmental parameters, while ensuring consistency, users can use only parts of the method to reduce the complexity if suitable data exists.

### 2.1 | Process simulation and techno-economic analysis

Next to designing new processes or modeling existing ones, process simulation in chemical engineering is used to generate mass and energy balance data of the relevant streams and unit operations of a process design to perform TEA. The process designs to be considered and analyzed have to be defined in the first stage and can be adjusted during process simulation iterations. While simple processes and flowsheets might be examined by hand calculation, process simulation tools are necessary to solve more complex problems and to supply a sufficient database for comprehensive analyses (Haydary, 2019).

Regarding potential applications, FT synthesis-based hydrocarbons and MeOH, besides the direct usage of green hydrogen, are seen as power-to-liquid products with a high chance of commercialization due to the potential to replace fossil-based production of base chemicals and fuels. FT synthesis products, MeOH, and their derivatives can substitute currently used products without or with minor application and infrastructure changes and are often called "drop-in" solutions (Schemme et al., 2020).

The applied process simulations aim to create reliable data on the production of (A) FT synthesis raw products and (B) MeOH by using mature technologies. The generated data is input for the subsequent techno-economic analysis, LCA, and the MOO. The techno-economic analysis aggregates detailed process steps into modules, providing relevant input/output correlations. Both chemical processes (A) and (B) are based on the supply of green hydrogen and gaseous CO_2. In (A), three product fractions are produced (naphtha, middle distillate, and wax) but are then brunched as one product. Further processing of the raw FT synthesis products could lead to higher-value products like SAF, diesel, and gasoline. Still, it would imply the need for additional equipment and a deeper investigation into the demand markets to find the optimal flowsheet design. Therefore, upgrading
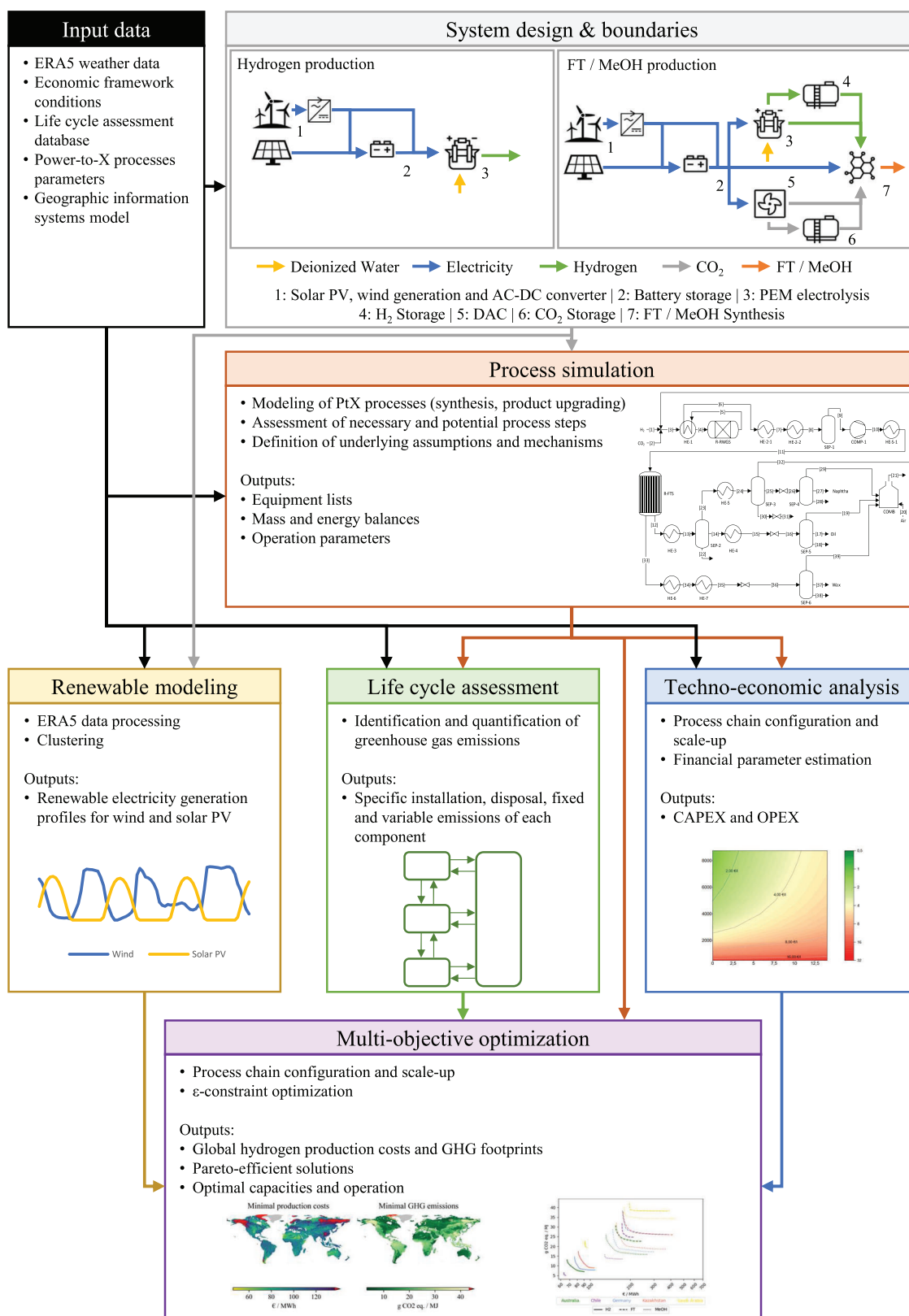
FIGURE 1 Graphical abstract of the multi-method approach.
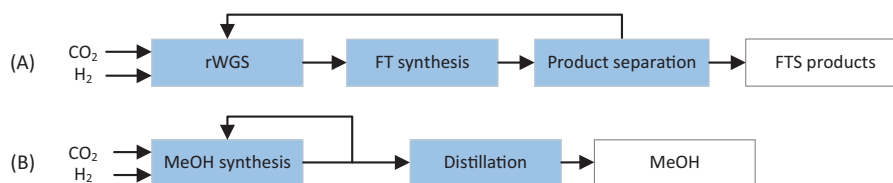
FIGURE 2 Simplified block flowsheet of the two synthesis process configurations: (a) FT synthesis-based process and (b) synthetic methanol-based process.

these raw products is outside the scope of this work. The same principle applies to process scheme (B), in which MeOH could be upgraded by applying further processes, but with the loss of generality of product application. Like in the current international structures, global trade will likely rely on primary product streams (currently petrol oil), and the upgrading or processing will be near the potential demanders.

The process setup for (A) relies on the supply of synthesis gas, a stoichiometric mixture of carbon monoxide (CO) and H_2, since the low-temperature FT synthesis applied in this work uses Cobalt (Co)-based catalysts that are not active for the conversion of CO_2 under relevant process conditions. To generate a suitable synthesis gas stream, CO_2 and H_2 are converted into synthesis gas by the reverse water gas shift reaction:

$$CO_2 + H_2 \rightleftharpoons CO + H_2O \quad \Delta_R H^0 = 41\,kJ/mol \tag{I}$$

The reverse water gas shift reaction is endothermic, so heat input is required. To prevent the formation of methane and carbon deposition (e.g., by the Boudouard reaction) while securing sufficient conversion, high-temperature levels of up to 1000°C are chosen. Due to the highest energy efficiency in a power-to-liquid FT synthesis process, an electrically heated reverse water gas shift reaction reactor is assumed.

In low-temperature FT synthesis reactors, *n*-paraffins are the main product. The reaction equation for the generation of *n*-paraffins by low-temperature FT synthesis can be simplified by assuming $(CH_2)_n$ as a *n*-paraffin with the chain length *n*:

$$CO + 2H_2 \rightarrow (CH_2)_n + H_2O \quad \Delta_R H^0 = -165\,kJ/mol \tag{II}$$

The process simulation assumes a particular product distribution according to the Anderson–Schulz–Flory distribution, using an alpha value of 0.9, referring to typical product distributions of low-temperature FT synthesis processes based on Co catalysts (Van De Loosdrecht et al., 2013).

For MeOH synthesis (B), no pre-processing of the incoming CO_2 and H_2 is necessary. The CO_2- and CO-based methanol synthesis reactions are represented by Equations (III) and (IV), with the consideration that the water gas shift reaction (V) and the reverse water gas shift reaction (I) is likely to occur as well, based on reactor conditions and composition:

$$CO_2 + 3H_2 \rightarrow CH_3OH + H_2O \quad \Delta_R H^0 = -49.2\,kJ/mol \tag{III}$$

$$CO + 2H_2 \rightarrow CH_3OH \quad \Delta_R H^0 = -90.8\,kJ/mol \tag{IV}$$

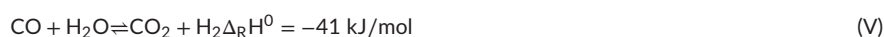$$CO + H_2O \rightleftharpoons CO_2 + H_2 \quad \Delta_R H^0 = -41\,kJ/mol \tag{V}$$

Figure 2 shows a simplified flowsheet for both processes (A) and (B):

While the estimation of production costs is in the scope of the optimization in this work, the applied method demands techno-economic input parameters derived from process simulations and the literature. The results of the process simulations provide the necessary data to estimate equipment cost. This is done either by using the built-in Aspen Plus Economic Analyzer for most of the equipment needed or by applying cost correlations and data from the literature, especially for specialized equipment. To update the cost estimation to a targeted reference time of 2023, the Chemical Engineering Plant Cost Index (CEPCI) was used. The application of surcharge factors is chosen to derive the entire capital investment, using the ratio factors from Peters et al. (2004) for fluid processing plants. Details about these cost calculations can be found in Section A3 of Supporting Information S1.

2.2 | Life cycle assessment

Heeding the ISO 14040 series, LCA is applied to evaluate the environmental burdens of the considered value chains. Since the global warming potential is one of the most relevant impact categories in today's cross-sectoral decision-making, this LCA focuses on identifying and quantifying

GHG emissions. The "cradle-to-gate" approach considers GHG emissions along the process chain from mining raw materials to the produced energy carrier (on the production site) and the end-of-life treatment of the waste flows.

The process chains for producing hydrogen, FT crude, and MeOH include RES-E, a battery, and proton exchange membrane (PEM) electrolysis. In addition, next to the synthesis units (c.f. Figure 2), the pathways for producing FT crude and MeOH comprise a direct air capture (DAC) unit and buffer tanks and compressors for the intermediates (H_2 and CO_2). The LCA aims to provide the MOO model's fixed and variable CO_2 emissions. Due to the optimization of the single process steps, no functional units for the entire product system are defined. Instead, every process step is represented by one reference unit (i.e., 1 MWh of H_2 storage capacity is the reference unit for the H_2 storage tank). Excess heat/steam as a by-product in the synthesis processes is used for internal heat demands in the DAC process. Since no additional by-products are generated, the consideration of allocations in the product system is omitted.

The life cycle inventory data is primarily from the process simulations and comprises energy and mass flows and utilities like electricity and cooling water (c.f. Section A4 of Supporting Information S1). Constructional data from LCA literature are used and extrapolated to the needed magnitude. The characteristics of further flows, like operating materials and emissions, are also obtained from the literature. Correspondingly to their importance in today's energy transition approaches, LCA data on water electrolysis (Bareiß et al., 2019; Gerloff, 2021; Palmer et al., 2021; Terlouw et al., 2022) and on DAC (Chauvy & Dubois, 2022; Deutz & Bardow, 2021; Madhu et al., 2021; Terlouw et al., 2021) are detailed in the literature. While numerous LCA studies on green MeOH production (Cordero-Lanzac et al., 2022; Hank et al., 2019; Sollai et al., 2023; Zhu et al., 2022) are described in the literature, studies on FT synthesis are less abundant (Micheli et al., 2022; Rojas-Michaga et al., 2023). Completing the life cycle inventory, the underlying supply chain and background data are drawn from the ecoinvent database 3.9.1 using the modeling software openLCA 2.0.2. The underlying supply chains are connected by market processes primarily for Europe, since interests and technical know-how surrounding PtX processes are predominantly concentrated in Europe, even for global implementations. To avoid the controversial issue of allocating waste flows, the system model "Allocation at the Point of Substitution" (APOS) was chosen (Wernet et al., 2016). Detailed information on data usage and calculation for life cycle inventory is provided in Section A4.2 of Supporting Information S1.

The global warming potential is the most suitable impact category in the frame of this work regarding the relevance of the carbon footprint of a product or process in today's decision-making in the transformation and defossilization of the energy and transport sector. ReCiPe 2016 v1.03, midpoint (H), as one of the state-of-the-art impact assessment methods, provides the climate change impact as defined by the Intergovernmental Panel on Climate Change (2013), including the CO_2-equivalent of the different GHGs with a residence time of 100 years (GWP100) (Huijbregts et al., 2017).

2.3 | Multi-objective optimization

The developed mixed-integer linear program is an extension of the model of Langenmayr and Ruppert (2023) and considers multiple objectives to obtain Pareto optimal solutions. These solutions contain optimal capacities and operation of PtX plants, allowing for a comprehensive assessment of resulting production costs and GHG emissions of derived PtX products. Sets of modeling constraints based on process simulation data ensure the appropriate implementation of technological processes. Economic and environmental data are incorporated into the model according to objective functions. Finally, the model allows for considering local data (e.g., weather conditions) to customize the process for specific locations. Whereas LCA and TEA define the system boundaries for the analysis, the optimization is performed for explicit case studies within the analysis scope. Such an approach is challenging to scale to numerous locations with individual properties like RES-E capacity factors. MOO considers each location's properties and economic and environmental data simultaneously, and determines optimal capacities and operations for each location. This makes MOO especially suitable for numerous locations with individual properties, as shown in the case studies presented in Section 3.3.

The first objective function (Equations 1 and 2) minimizes the annual total costs of the PtX processes, which consist of the annualized investment (*ANN*), yearly fixed maintenance and operation costs (*FOM*), variable maintenance and operation costs (*VOM*) of each component k, and dispatch costs from the purchase, selling, and disposal of each commodity c, and start-up costs of components (*SU*). Investment i also includes renewed investments in components after their service life and residual values of components at the end of the PtX plant's service life.

$$\text{Total costs} = \sum_k \left(i_k \left(\text{ANN}_k + \text{FOM}_k \right) + \text{SU}_k + \sum_c \sum_t x^{\text{out}}_{k,s^{MO}(k),c,t} \cdot \text{VOM}_k \cdot W_c \right) + \sum_{s^S} \left(i_{s^S} \left(\text{ANN}_{s^S} + \text{FOM}_{s^S} \right) + \sum_c \sum_t x^{\text{charge}}_{s^S,c,t} \cdot \text{VOM}_{s^S} \cdot W_c \right)$$

$$+ \sum_g \left(i_g \left(\text{ANN}_g + \text{FOM}_g \right) + \sum_c \sum_t x^{\text{generation}}_{g,s^G(g),c,t} \cdot \text{VOM}_g \cdot W_c \right) + \sum_c \sum_t \left(\sum_{s^P} x^{\text{purchase}}_{s^P,c,t} \cdot P^{\text{purchase}}_{s^P,c,t} - \sum_{s^Q} x^{\text{sell}}_{s^Q,c,t} \cdot P^{\text{sell}}_{s^Q,c,t} \right) \cdot W_c \quad (1)$$

$$f_1 = \min \text{Total costs} \quad (2)$$

The second objective function (Equations and 4) minimizes the annual total GHG emissions of the PtX processing plant. Carbon footprints are considered in the installation of the components ($GF^{\text{installation}}$), the fixed annual operation and maintenance (GF^{FOM}), the variable operation and maintenance (GF^{VOM}), and the disposal of the components (GF^{disposal}).). In addition, the GHG footprint of purchased (GF^{purchase}) and sold (GF^{sell}) commodities are also considered.

$$
\begin{aligned}
\text{Total emissions} = &\sum_k \left(cap_k \left(GF_k^{\text{installation}} + GF_k^{\text{disposal}} + GF_k^{\text{fixed O\&M}} \right) + \sum_c \sum_t x_{k,s^{MO}(k),c,t}^{\text{out}} \cdot GF_k^{\text{variable O\&M}} \cdot W_c \right) \\
+ &\sum_{s^S} \left(cap_{s^S} \left(GF_{s^S}^{\text{installation}} + GF_{s^S}^{\text{disposal}} + GF_{s^S}^{\text{fixed O\&M}} \right) + \sum_c \sum_t x_{s^S,c,t}^{\text{charge}} \cdot GF_{s^S}^{\text{variable O\&M}} \cdot W_c \right) \\
+ &\sum_g \left(cap_g \left(GF_g^{\text{installation}} + GF_g^{\text{disposal}} + GF_g^{\text{fixed O\&M}} \right) + \sum_c \sum_t x_{g,s^G(g),c,t}^{\text{generation}} \cdot GF_{s^G(g)}^{\text{variable O\&M}} \cdot W_c \right) \\
+ &\sum_c \sum_t \left(\sum_{s^P} x_{s^P,c,t}^{\text{purchase}} \cdot GF_s^{\text{purchase}} - \sum_{s^Q} x_{s^Q,c,t}^{\text{sell}} \cdot GF_{s^Q}^{\text{sell}} \right) \cdot W_c
\end{aligned}
\tag{3}
$$

$$
f_2 = \min \text{Total emissions}
\tag{4}
$$

In this work, MOO combines both objective functions simultaneously to investigate the relation between costs and GHG emissions. Based on the work of Mavrotas (2009), the first step calculates the payoff table. In this payoff table, the result of f_2 when minimizing f_2 represents the GHG emission utopia value, and the result of minimizing f_2 when first minimizing f_1 represents the GHG emission nadir value approximation. We calculate the range between utopia and nadir value approximation, and separate the range into 100 intervals. In the second step, we incorporate the intervals in the optimization problem by adjusting f_1 and add a new constraint to consider the interval step.

$$
f_1 = \min \left(\text{Total costs} - \text{slack} \cdot \varepsilon \right)
\tag{5}
$$

$$
\text{Total emissions} + \text{slack} - e_i = 0
\tag{6}
$$

The constraint in Equation (6) ensures that the total emissions are lower than or equal to the precalculated interval value e_i. Using the slack variable in the objective function Equation (5) and in Equation (6), we ensure only efficient solutions are taken. The impact of the slack variable on the objective function is minimal since the epsilon coefficient is an adequately small number.

The constraints of the MOO represent the technical properties of the conversion units, like ramping abilities, minimal and maximal loads, and efficiencies. In addition, storage units are considered by defining their state of charge, minimal and maximal state of charge, charging and discharging efficiencies, charging and discharging power, and power-to-capacity ratios. Finally, generator units use hourly capacity factors and the capacity variable to calculate the hourly RES-E generation. Constraints concerning commodities define the option to buy, sell, emit, and obtain the individual commodity or to set total yearly demand, which the optimized PtX plant must cover. Next to technical properties, economic and environmental data are connected to the optimization problem, like scaling factors, CAPEX, and market data (purchase and selling prices and emissions). Since the setup of components and utilized options, such as purchasing and selling commodities, can be individually adjusted, the model applies to manifold processes and case studies. The complete model is presented in Section A5.1 of Supporting Information S1.

3 | RESULTS

The following section contains an excerpt of the process simulation, TEA, and LCA results. The main results stem from the MOO, which consists of a global view of green hydrogen production, a location-specific analysis of the relationship between production costs and GHG emissions, and investment decision support for the PtX production of hydrogen, FT, and MeOH. Comprehensive information and results on the other applied methods can be found in Sections A3.3, A3.5, and A4.3 of Supporting Information S1.

TABLE 1 Key results of the process simulations and the techno-economic analysis.

Parameter	(A) FT	(B) MeOH
Input	0.439 kg H_2	0.191 kg H_2
	3.138 kg CO_2	1.395 kg CO_2
	4.386 kWh electricity	0.314 kWh electricity
Output	1 kg FT crude	1 kg MeOH
I_0	167,865,923€	118,669,824€
C_0	22,767 kg_{FT}/h	52,312 kg_{MeOH}/h
δ	0.67	0.67

TABLE 2 Fixed and variable GHG emissions from life cycle assessment used in the optimization model.

Processes	Fixed emissions per capacity $GF^{installation} + GF^{FOM} + GF^{disposal}$		Variable emissions per output GF^{VOM}	
Wind turbine	1,115	kg CO_{2eq} per kW	0.19	kg CO_{2eq} per MWh
PV system	2,398	kg CO_{2eq} per kW	0.00002	kg CO_{2eq} per MWh
PEM electrolysis	114	kg CO_{2eq} per kW input	0.0009	kg CO_{2eq} per kWh input
H_2 compressor	394	kg CO_{2eq} per kg H_2/h	0	kg CO_{2eq} per kg H_2
DAC unit	18.8	kg CO_{2eq} per kg CO_2/h	0.0476	kg CO_{2eq} per kg CO_2
CO_2 compressor	2.7	kg CO_{2eq} per kg CO_2/h	0	kg CO_{2eq} per kg CO_2
FT synthesis	6,146	kg CO_{2eq} per kg FT crude/h	0.094	kg CO_{2eq} per kg FT crude
MeOH synthesis	2,685	kg CO_{2eq} per kg MeOH/h	0.028	kg CO_{2eq} per kg MeOH
LFP battery	105,645	kg CO_{2eq} per MWh	0	kg CO_{2eq} per MWh
H_2 storage vessel	69,270	kg CO_{2eq} per t H_2	0	kg CO_{2eq} per t H_2
CO_2 storage vessel	1,598	kg CO_{2eq} per t CO_2	0	kg CO_{2eq} per t CO_2

3.1 | Results of process simulation

For the MOO, the normalized inputs and outputs are of interest, as well as the investment I_0 needed for a base capacity C_0 sized synthesis unit and, if applicable, a scaling exponent δ, which adjusts the investment I to the actual capacity C by taking into account economies of scale, as displayed in Equation (7). The investment I can be calculated based on different capacities C, resulting in an investment curve. This curve is linearized into segments (c.f. Section A5.2 of Supporting Information S1) and integrated into the MOO to calculate the specific investment i_k of each component (Equation 1).

$$\frac{I}{I_0} = \left(\frac{C}{C_0}\right)^{\delta} \tag{7}$$

Table 1 sums up the process simulation and economic analysis results. The results are based on a steady-state simulation of a PtX plant with an input of 10 t/h H_2.

3.2 | Results of life cycle assessment

The MOO model needs the one-time emissions associated with the plant and site construction ($GF^{installation}$, GF^{FOM}, and $GF^{disposal}$) and the ongoing emissions (GF^{VOM}) (Equation 3). Thus, the results are divided into fixed and variable emissions, as shown in Table 2. Since disposal efforts per unit occur only once, their resulting emissions are also included in the fixed emissions. Additional information on the results, their sensitivity, and the validity of the LCA are discussed in Section A4.3 of Supporting Information S1.
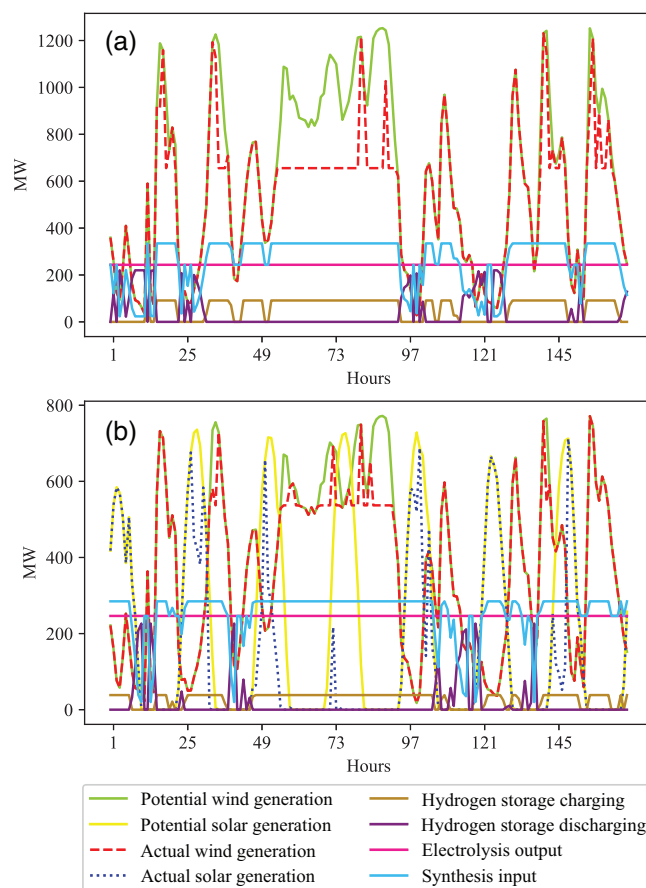
FIGURE 3 Interplay between components having green hydrogen as input or output and renewable electricity supply in the case of environmental (a) and economic (b) optimization of FT production in Australia. Numerical data of the figure is given in Supporting Information S2.

3.3 | Results of the dynamic multi-objective optimization

We apply the MOO to the production of hydrogen, FT, and MeOH in five different locations (longitude and latitude): Chile (−71.00°, −53.00°), Australia (127.75°, −30.75°), Germany (8.78°, 53.75°), Kazakhstan (50.00°, 48.50°), and Saudi Arabia (36.50°, 28.50°). These locations were chosen to analyze the impact of different CFs: Chile has excellent wind conditions, Saudi Arabia has excellent PV conditions, and Germany, Australia, and Kazakhstan have mixed CFs. In the case of hydrogen, we additionally supply a global view on minimal production costs and GHG emissions. Eleven years of weather data for each location are obtained from the ERA 5 (Hersbach et al., 2020) dataset and processed with the open-source tool atlite (Hofmann et al., 2021) to capacity factor profiles of the RES-E generators. The wind capacity factor profiles include losses from AC to DC conversion. The clustering of the data is described in Langenmayr and Ruppert (2023). Next to synthesis and PEM electrolysis, we include battery, hydrogen, and CO_2 storage, as well as necessary compressors. The CO_2 is obtained from a low-temperature DAC. Techno-economic assumptions, which the process simulations have not covered, are provided in Tables 13–15 of Supporting Information S1.

The electricity supply of the PtX plants stems from using wind and solar PV electricity generation. Based on the hourly CF, the capacities of all components are dimensioned to achieve a sufficient and secure supply of all conversion components in the plant. In addition, the operation of the system is optimized. Figure 3 showcases an excerpt of the operation of FT production in Australia in the case of GHG emissions (A) and production costs (B) minimization. The figure clearly shows how components interact with each other hourly and how different objectives affect the choice of components and the operation.

3.3.1 | A global view of green hydrogen production

Our approach allows for a two-fold analysis. First, large areas for PtX implementations can be considered based on high-resolution geographical data. The maps in Figure 4 show the results of production costs and GHG emissions minimization on a global scale. This map can be used to get a
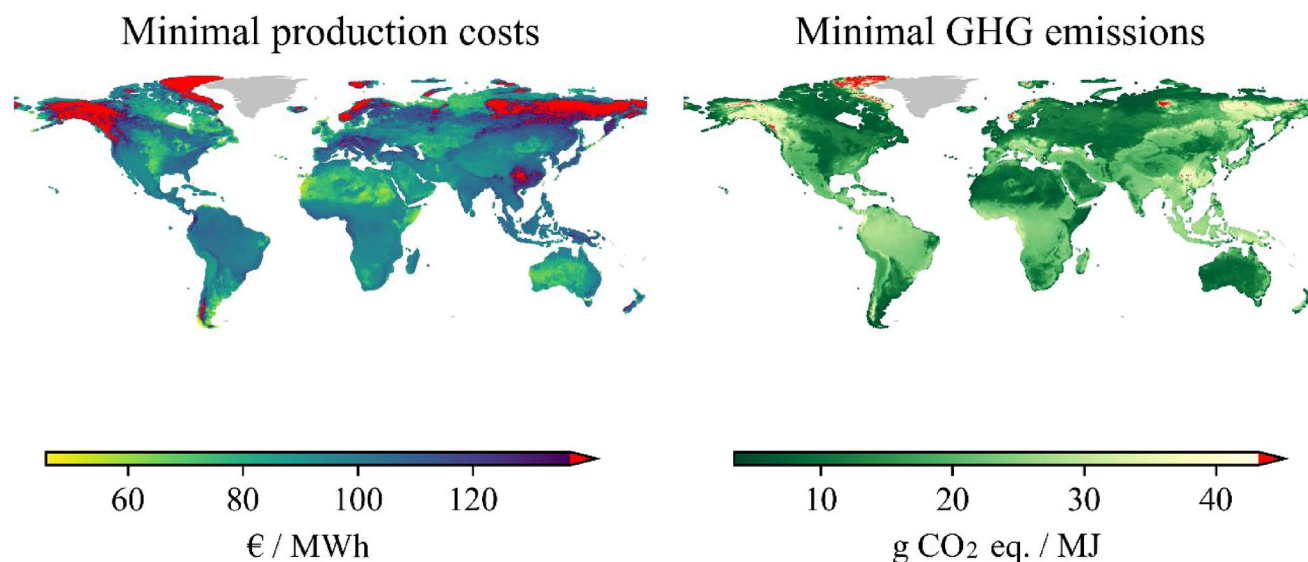
FIGURE 4 Minimal hydrogen production costs (left) and minimal GHG emissions of hydrogen production (right). Production cost and GHG emission outliers of the results are colored in red to reduce their impact on the scales. Numerical data of the figure is given in Supporting Information S2.
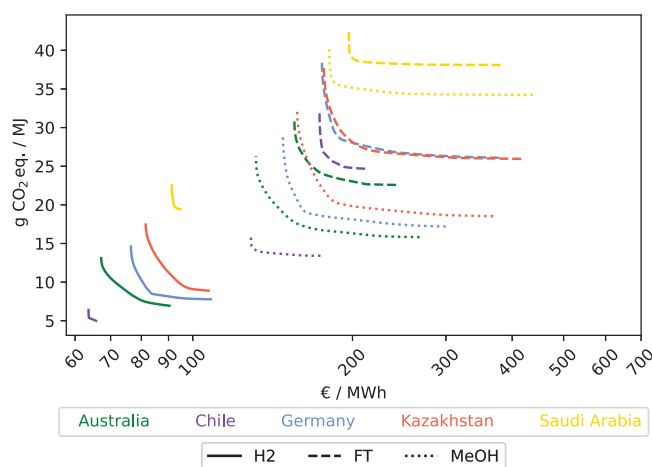

FIGURE 5 Pareto fronts for the chosen locations for producing renewable hydrogen. Numerical data of the figure is given in Supporting Information S2.

general overview of suitable PtX regions concerning minimal costs and GHG emissions. When production costs are minimized, the costs range from 45.73 to 443.42€/MWh, and in the case of GHG emission minimization, the emissions range from 3.45 to 76.68 g CO_{2eq}./MJ.

3.3.2 | Detailed analysis of suitable PtX plant locations

Figure 5 shows the technology and location-specific Pareto fronts derived from the MOO. Looking at the hydrogen production Pareto fronts, it is visible that the location of Chile (CF wind: 5,093 h; CF solar: 1,116 h) performs best concerning GHG emissions and costs compared to the other locations in the case of hydrogen and MeOH production. The Pareto front in Chile is relatively narrow compared to different locations and technologies, showing that production costs and GHG emissions are predominantly aligned. As soon as locations increasingly use solar PV for electricity generation, the Pareto fronts start steeply increasing GHG emissions when aiming for lower production costs. The LCA results show that solar PV has higher GHG emissions per installed capacity than wind generation, and using solar PV to decrease production costs heavily increases GHG emissions. However, locations with mixed capacity factors, Germany (CF wind: 3,532 h; CF solar: 1,084 h), Australia (CF wind: 3,447 h; CF solar: 1,752 h), and Kazakhstan (CF wind: 2,684 h; CF solar: 1,241 h), can replace the majority of GHG emissions without significant increase of costs since
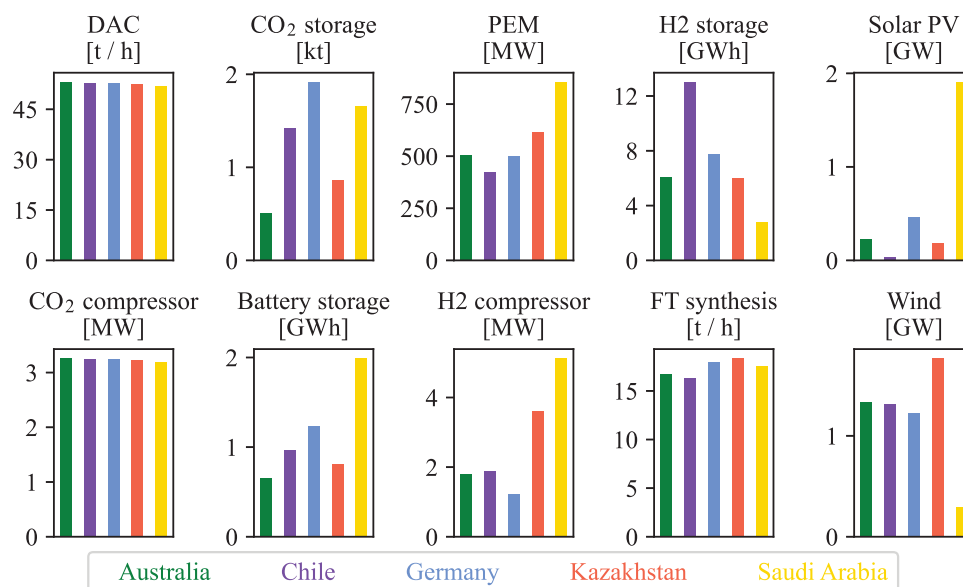
FIGURE 6 Capacities of all components of the Fischer–Tropsch production in different countries using the best trade-off capacities. Numerical data of the figure is given in Supporting Information S2.

replacing solar PV with wind generation in combination with battery storage is sufficient to cover the electricity demand. The advantage of diversification of electricity generation is less pronounced for the location of Saudi Arabia (CF wind: 1,026 h; CF solar: 1,956 h). Significant amounts of wind generation must be installed to reduce solar PV generation, increasing production costs and shortening the steep increase of GHG emissions.

Several challenges accompany the synthesis of green hydrogen into hydrogen derivatives. First, other commodities like CO_2 or heat are needed as input, next to electricity. Second, synthesis units are less flexible than PEM electrolysis, and a steady supply of inputs is necessary, which contradicts the volatile character of renewable energy. Therefore, the integration of renewable electricity is more demanding. The capital investment into the different synthesis technologies and the DAC units, in combination with overcapacities and storage units, to allow for a steady supply of inputs, results in higher costs. Like costs, GHG emissions also increase for the same reasons. The substantial cost increase is evident if the lowest possible GHG emissions are achieved. This circumstance emphasizes the need to consider both objectives when investing in hydrogen and its derivatives to avoid costly GHG abatement strategies. Comparing the course of the Pareto fronts of FT and MeOH shows an interesting aspect. While Chile's hydrogen and MeOH fronts perform better in terms of costs and emissions than all other countries, the FT front of Chile performs worse than the FT Pareto front in Australia. The reduced flexibility of the FT synthesis challenges electricity generation mainly from wind, resulting in additional auxiliary component capacities. Australia has good mixed capacity factors and can combine solar PV and wind generation capacities to supply more steady electricity.

Regarding the production costs of hydrogen as a product, the best-performing scenario (Chile) is reaching minimum costs close to the often-referred fossil reference threshold of 72€/MWh (2$/kg) (IEA, 2024). Methanol and FT crude production costs in the economically best-performing scenarios (Chile and Australia, respectively) are higher than their fossil references by a factor of three to four (Arnaiz Del Pozo et al., 2022; Hafner, 2022; IRENA and Methanol Institute, 2021; Oil & Energy Trends, 2024). The GHG emissions associated with fossil hydrogen production from natural gas or coal far exceed those of green hydrogen, even when carbon capture and storage are included. However, comparing the renewable hydrocarbon products MeOH and FT crude with their fossil references is difficult, as negative GHG emissions from DAC should be included. A more detailed comparison of the results with their fossil reference products can be found in Section A6.3 of Supporting Information S1.

The advantage of Pareto fronts is that trade-offs between production costs and GHG emissions are displayed, and investors can choose the Pareto solution that best fits their preferences regarding costs and emissions. In addition, for each trade-off, the MOO provides optimal capacities for all components and operational information to support the investment decision. Suppose a balanced relation between production costs and GHG emissions is admired. In that case, the trade-off of the Pareto front closest to the origin of the normalized coordinate system presents an appropriate choice. Using this balanced trade-off, Figure 6 shows the installed capacity, the primary decision in PtX investment, per location to produce FT. It highlights how the different CFs affect the generation unit's choice and all components' capacities. For example, the location in Saudi Arabia exploits high solar PV availability by installing large capacities of solar PV generation in combination with battery storage capacities, since solar PV can only provide a steady electricity supply during the day when storages are charged, but nighttime needs to be covered without RES-E generation. In contrast, Chile dismisses solar PV capacities since wind generation substitutes for all solar PV generation due to sufficient wind CFs. Further results and a sensitivity analysis are given in Section A6 of Supporting Information S1.

4 | SUMMARY, CONCLUSION, AND FUTURE WORK

PtX processes connect the electricity sector with other sectors like heating, transportation, and industry. This holds the opportunity to enable the energy transition toward sectoral defossilization. In the presented multi-method approach, we combined process simulations with techno-economic analysis and LCA to analyze different PtX products. The technology paths are modeled in detail by integrating necessary equipment, mass and energy balances, and economic and environmental parameters. The derived comprehensive data on producing green hydrogen, FT crude, and MeOH were applied in a dynamic MOO tool designed to model and optimize PtX pathways. The developed approach allows the determination of location-specific production costs and emissions, enables the trade-off analysis between both objectives based on optimized capacities, and successfully overcomes the limitations of the single-method approaches as commonly applied in the reviewed literature.

Our results show that wind generation is advantageous compared to solar PV generation for two reasons: First, wind electricity generation can achieve higher capacity factors, resulting in low-cost electricity generation. Second, the LCA shows that wind generation has lower specific GHG emissions per installed capacity, providing an environmental advantage compared to solar power generation. Therefore, regions with excellent wind conditions, like Patagonia in southern Chile, enable low-cost and low-emission production of renewable hydrogen and hydrogen derivatives. From a global perspective, locations with mixed renewable availability, such as Australia, Germany, and Kazakhstan, benefit from substituting wind with solar PV generation or vice versa to achieve either low-emission or low-cost production. Locations with high solar PV but low wind availability, like Saudi Arabia, show higher emissions in the production processes since large quantities of wind capacity have to be installed to reduce emissions. Based on the obtained Pareto fronts, investment decisions can be taken, and optimal capacities and operations can be determined to allow comparison of trade-off solutions. By comparing the different PtX energy carriers, we see that hydrogen performs best since auxiliary components to support the inflexible synthesis operation, like storage units, have lower capacities, and additional feedstock like CO_2 is unnecessary. The performance of FT and MeOH processes shows that individual characteristics like flexibility or heat demand derived from comprehensive process simulations affect production costs and emissions at each location individually, emphasizing the necessity for in-depth analysis and consideration of such parameters.

Even though we used an extensive multi-method approach to assess PtX processes, some methodological limitations exist. For example, uncertainties from RES-E or the PtX processes are not considered. Stochastic or robust optimization could be applied to consider such parameter uncertainties in future works. For the LCA, fixed capacities are assumed, which contradicts the variable capacities in the optimization model. Hence, conducting the LCA for different capacities could help to consider scaling effects and provide better GHG emission results. In addition, other impact categories could be included, such as water consumption or land use. Furthermore, the LCA heavily relies on life cycle inventory data, mainly affecting solar PV emissions. Long-term developments, such as producing solar PV modules with renewable electricity, are not considered in the data but could significantly reduce PV module production emissions. Furthermore, a more detailed process simulation of components could improve the modeling in the optimization context. For example, PEM electrolysis efficiency depends on the current power level and can exceed its nominal capacities for the short term. Finally, the multi-model approach only assesses the production of PtX products. However, it does not consider other important aspects such as transportation and infrastructure, water availability, or political conditions, which will further affect costs and GHG emissions and provide investment decision support.

AUTHOR CONTRIBUTIONS

ACKNOWLEDGMENTS

CONFLICT OF INTEREST STATEMENT

The authors declare no conflicts of interest.

DECLARATION OF GENERATIVE AI AND AI-ASSISTED TECHNOLOGIES

To improve the readability of our work, we have applied Grammarly (v.1.2.92.1464).

DATA AVAILABILITY STATEMENT

The multi-objective optimization has been implemented in Python and is available as open source here: https://github.com/ulicious/ptx_now. All data to recreate the results in this manuscript are published with a CC by 4.0 license and can be found in Langenmayr (2025).

ORCID

Uwe Langenmayr [iD] https://orcid.org/0000-0002-3436-7228

REFERENCES

Albrecht, F. G., König, D. H., Baucks, N., & Dietrich, R.-U. (2017). A standardized methodology for the techno-economic evaluation of alternative fuels—A case study. *Fuel*, *194*, 511–526. https://doi.org/10.1016/j.fuel.2016.12.003

Armijo, J., & Philibert, C. (2020). Flexible production of green hydrogen and ammonia from variable solar and wind energy: Case study of Chile and Argentina. *International Journal of Hydrogen Energy*, *45*(3), 1541–1558. https://doi.org/10.1016/j.ijhydene.2019.11.028

Arnaiz Del Pozo, C., Cloete, S., & Jiménez Álvaro, Á. (2022). Techno-economic assessment of long-term methanol production from natural gas and renewables. *Energy Conversion and Management*, *266*, 115785. https://doi.org/10.1016/j.enconman.2022.115785

Bareiß, K., de la Rua, C., Möckl, M., & Hamacher, T. (2019). Life cycle assessment of hydrogen from proton exchange membrane water electrolysis in future energy systems. *Applied Energy*, *237*, 862–872. https://doi.org/10.1016/j.apenergy.2019.01.001

Berger, M., Radu, D., Detienne, G., Deschuyteneer, T., Richel, A., & Ernst, D. (2021). Remote renewable hubs for carbon-neutral synthetic fuel production. *Frontiers in Energy Research*, *9*, 671279. https://doi.org/10.3389/fenrg.2021.671279

Campos-Guzmán, V., García-Cáscales, M. S., Espinosa, N., & Urbina, A. (2019). Life cycle analysis with multi-criteria decision making: A review of approaches for the sustainability evaluation of renewable energy technologies. *Renewable and Sustainable Energy Reviews*, *104*, 343–366. https://doi.org/10.1016/j.rser.2019.01.031

Chauvy, R., & Dubois, L. (2022). Life cycle and techno-economic assessments of direct air capture processes: An integrated review. *International Journal of Energy Research*, *46*(8), 10320–10344. https://doi.org/10.1002/er.7884

European Union. (2023). Commission Delegated Regulation (EU) 2023/1184 of 10 February 2023 Supplementing Directive (EU) 2018/2001 of the European Parliament and of the Council by Establishing a Union Methodology Setting out Detailed Rules for the Production of Renewable Liquid and Gaseous Transport Fuels of Non-Biological Origin, 2023/1184. https://eur-lex.europa.eu/legal-content/EN/TXT/PDF/?uri=CELEX:32023R1184

Cordero-Lanzac, T., Ramirez, A., Navajas, A., Gevers, L., Brunialti, S., Gandía, L. M., Aguayo, A. T., Sarathy, S. M., & Gascon, J. (2022). A techno-economic and life cycle assessment for the production of green methanol from CO_2: Catalyst and process bottlenecks. *Journal of Energy Chemistry*, *68*, 255–266. https://doi.org/10.1016/j.jechem.2021.09.045

De Klerk, A. (2008). Fischer–Tropsch refining: Technology selection to match molecules. *Green Chemistry*, *10*(12), 1249. https://doi.org/10.1039/b813233j

Deutz, S., & Bardow, A. (2021). Life-cycle assessment of an industrial direct air capture process based on temperature–vacuum swing adsorption. *Nature Energy*, *6*(2), 203–213. https://doi.org/10.1038/s41560-020-00771-9

Dry, M. E. (1999). Fischer–Tropsch reactions and the environment. *Applied Catalysis A: General*, *189*(2), 185–190. https://doi.org/10.1016/S0926-860X(99)00275-6

Farajiamiri, M., Meyer, J.-C., & Walther, G. (2023). Multi-objective optimization of renewable fuel supply chains regarding cost, land use, and water use. *Applied Energy*, *349*, 121652. https://doi.org/10.1016/j.apenergy.2023.121652

Fasihi, M., Bogdanov, D., & Breyer, C. (2016). Techno-economic assessment of power-to-liquids (PtL) fuels production and global trading based on hybrid PV-wind power plants. *Energy Procedia*, *99*, 243–268. https://doi.org/10.1016/j.egypro.2016.10.115

Gerloff, N. (2021). Comparative life-cycle-assessment analysis of three major water electrolysis technologies while applying various energy scenarios for a greener hydrogen production. *Journal of Energy Storage*, *43*, 102759. https://doi.org/10.1016/j.est.2021.102759

Götz, M., Lefebvre, J., Mörs, F., McDaniel Koch, A., Graf, F., Bajohr, S., Reimert, R., & Kolb, T. (2016). Renewable power-to-gas: A technological and economic review. *Renewable Energy*, *85*, 1371–1390. https://doi.org/10.1016/j.renene.2015.07.066

Hafner, M., (with Luciani, G.). (2022). *The Palgrave handbook of international energy economics*. Springer International Publishing AG.

Hank, C., Lazar, L., Mantei, F., Ouda, M., White, R. J., Smolinka, T., Schaadt, A., Hebling, C., & Henning, H.-M. (2019). Comparative well-to-wheel life cycle assessment of OME 3–5 synfuel production via the power-to-liquid pathway. *Sustainable Energy & Fuels*, *3*(11), 3219–3233. https://doi.org/10.1039/C9SE00658C

Haydary, J., (with American Institute of Chemical Engineers). (2019). *Chemical process design and simulation: Aspen Plus and Aspen HYSYS applications*. Wiley.

Heinzmann, P., Glöser-Chahoud, S., Dahmen, N., Langenmayr, U., & Schultmann, F. (2021). *Techno-ökonomische Bewertung der Produktion regenerativer synthetischer Kraftstoffe*. Karlsruher Institut für Technologie (KIT). https://doi.org/10.5445/IR/1000140638

Hersbach, H., Bell, B., Berrisford, P., Hirahara, S., Horányi, A., Muñoz-Sabater, J., Nicolas, J., Peubey, C., Radu, R., Schepers, D., Simmons, A., Soci, C., Abdalla, S., Abellan, X., Balsamo, G., Bechtold, P., Biavati, G., Bidlot, J., Bonavita, M., … Thépaut, J. (2020). The ERA5 global reanalysis. *Quarterly Journal of the Royal Meteorological Society*, *146*(730), 1999–2049. https://doi.org/10.1002/qj.3803

Hofmann, F., Hampp, J., Neumann, F., Brown, T., & Hörsch, J. (2021). atlite: A lightweight Python package for calculating renewable power potentials and time series. *Journal of Open Source Software*, *6*(62), Article 62. https://doi.org/10.21105/joss.03294

Hoppe, W., Thonemann, N., & Bringezu, S. (2018). Life cycle assessment of carbon dioxide–based production of methane and methanol and derived polymers. *Journal of Industrial Ecology*, *22*(2), 327–340. https://doi.org/10.1111/jiec.12583

Huijbregts, M. A. J., Steinmann, Z. J. N., Elshout, P. M. F., Stam, G., Verones, F., Vieira, M., Zijp, M., Hollander, A., & van Zelm, R. (2017). ReCiPe2016: A harmonised life cycle impact assessment method at midpoint and endpoint level. *The International Journal of Life Cycle Assessment*, *22*(2), 138–147. https://doi.org/10.1007/s11367-016-1246-y

International Energy Agency (IEA). (2021). *Ammonia technology roadmap: Towards more sustainable nitrogen fertiliser production*. OECD. https://doi.org/10.1787/f6daa4a0-en

International Energy Agency (IEA). (2023). *Global hydrogen review 2023*. OECD. https://doi.org/10.1787/cb2635f6-en

International Energy Agency (IEA). (2024). *Global hydrogen eeview 2024*. IEA. https://www.iea.org/reports/global-hydrogen-review-2024

IRENA and Methanol Institute. (2021). Innovation Outlook : Renewable Methanol, International Renewable Energy Agency, Abu Dhabi.

Jacobasch, E., Herz, G., Rix, C., Müller, N., Reichelt, E., Jahn, M., & Michaelis, A. (2021). Economic evaluation of low-carbon steelmaking via coupling of electrolysis and direct reduction. *Journal of Cleaner Production*, *328*, 129502. https://doi.org/10.1016/j.jclepro.2021.129502

Kadam, R. S., & Yadav, G. D. (2024). Life cycle analysis of ammonia and methane production using green hydrogen and carbon dioxide. *Journal of Cleaner Production*, *449*, 141620. https://doi.org/10.1016/j.jclepro.2024.141620

Kenkel, P., Wassermann, T., Rose, C., & Zondervan, E. (2021). A generic superstructure modeling and optimization framework on the example of bi-criteria Power-to-Methanol process design. *Computers & Chemical Engineering*, *150*, 107327. https://doi.org/10.1016/j.compchemeng.2021.107327

Koj, J. C., Wulf, C., & Zapp, P. (2019). Environmental impacts of power-to-X systems—A review of technological and methodological choices in life cycle assessments. *Renewable and Sustainable Energy Reviews*, *112*, 865–879. https://doi.org/10.1016/j.rser.2019.06.029

Langenmayr, U. (2025). *Location-specific renewable profiles and Power-to-X parameters*. Zenodo. https://doi.org/10.5281/ZENODO.14848855

Langenmayr, U., & Ruppert, M. (2023). *Calculation of synthetic energy carrier production costs with high temporal and geographical resolution*. Karlsruher Institut für Technologie (KIT). https://doi.org/10.5445/IR/1000162460

Lee, H., Choe, B., Lee, B., Gu, J., Cho, H.-S., Won, W., & Lim, H. (2022). Outlook of industrial-scale green hydrogen production via a hybrid system of alkaline water electrolysis and energy storage system based on seasonal solar radiation. *Journal of Cleaner Production*, *377*, 134210. https://doi.org/10.1016/j.jclepro.2022.134210

Madhu, K., Pauliuk, S., Dhathri, S., & Creutzig, F. (2021). Understanding environmental trade-offs and resource demand of direct air capture technologies through comparative life-cycle assessment. *Nature Energy*, *6*(11), 1035–1044. https://doi.org/10.1038/s41560-021-00922-6

Maggi, A., Wenzel, M., & Sundmacher, K. (2020). Mixed-integer linear programming (MILP) approach for the synthesis of efficient power-to-syngas processes. *Frontiers in Energy Research*, *8*, 161. https://doi.org/10.3389/fenrg.2020.00161

Mavrotas, G. (2009). Effective implementation of the ε-constraint method in multi-objective mathematical programming problems. *Applied Mathematics and Computation*, *213*(2), 455–465. https://doi.org/10.1016/j.amc.2009.03.037

Micheli, M., Moore, D., Bach, V., & Finkbeiner, M. (2022). Life-cycle assessment of power-to-liquid kerosene produced from renewable electricity and CO_2 from direct air capture in Germany. *Sustainability*, *14*(17), 10658. https://doi.org/10.3390/su141710658

Morgan, E. R., Manwell, J. F., & McGowan, J. G. (2017). Sustainable ammonia production from U.S. offshore wind farms: A techno-economic review. *ACS Sustainable Chemistry & Engineering*, *5*(11), 9554–9567. https://doi.org/10.1021/acssuschemeng.7b02070

Oil and Energy Trends. (2024). Prices. *Oil and Energy Trends*, *49*(7–8), 52–54. https://doi.org/10.1111/oet.9_13128

Osman, O., Sgouridis, S., & Sleptchenko, A. (2020). Scaling the production of renewable ammonia: A techno-economic optimization applied in regions with high insolation. *Journal of Cleaner Production*, *271*, 121627. https://doi.org/10.1016/j.jclepro.2020.121627

Oyewo, A. S., Lopez, G., ElSayed, M., Galimova, T., & Breyer, C. (2024). Power-to-X economy: Green e-hydrogen, e-fuels, e-chemicals, and e-materials opportunities in Africa. *Energy Reports*, *12*, 2026–2048. https://doi.org/10.1016/j.egyr.2024.08.011

Palmer, G., Roberts, A., Hoadley, A., Dargaville, R., & Honnery, D. (2021). Life-cycle greenhouse gas emissions and net energy assessment of large-scale hydrogen production via electrolysis and solar PV. *Energy & Environmental Science*, *14*(10), 5113–5131. https://doi.org/10.1039/D1EE01288F

Peters, M. S., Timmerhaus, K. D., West, R. E., & West, R. E. (2004). *Plant design and economics for chemical engineers* (5th ed., international ed. 2004). McGraw-Hill. ISBN: 0-07-0496137-7.

Rego de Vasconcelos, B., & Lavoie, J.-M. (2019). Recent advances in power-to-X technology for the production of fuels and chemicals. *Frontiers in Chemistry*, *7*, 392. https://doi.org/10.3389/fchem.2019.00392

Rojas-Michaga, M. F., Michailos, S., Cardozo, E., Akram, M., Hughes, K. J., Ingham, D., & Pourkashanian, M. (2023). Sustainable aviation fuel (SAF) production through power-to-liquid (PtL): A combined techno-economic and life cycle assessment. *Energy Conversion and Management*, *292*, 117427. https://doi.org/10.1016/j.enconman.2023.117427

Runge, P., Sölch, C., Albert, J., Wasserscheid, P., Zöttl, G., & Grimm, V. (2020). Economic comparison of electric fuels produced at excellent locations for renewable energies: A scenario for 2035. *SSRN Electronic Journal*. https://doi.org/10.2139/ssrn.3623514

Schack, D., Rihko-Struckmann, L., & Sundmacher, K. (2016). Structure optimization of power-to-chemicals (P2C) networks by linear programming for the economic utilization of renewable surplus energy. In *Computer aided chemical engineering* (Vol. 38, pp. 1551–1556). Elsevier. https://doi.org/10.1016/B978-0-444-63428-3.50263-0

Schemme, S., Breuer, J. L., Köller, M., Meschede, S., Walman, F., Samsun, R. C., Peters, R., & Stolten, D. (2020). H_2-based synthetic fuels: A techno-economic comparison of alcohol, ether and hydrocarbon production. *International Journal of Hydrogen Energy*, *45*(8), 5395–5414. https://doi.org/10.1016/j.ijhydene.2019.05.028

Schmidt, P., Batteiger, V., Roth, A., Weindorf, W., & Raksha, T. (2018). Power-to-liquids as renewable fuel option for aviation: A review. *Chemie Ingenieur Technik*, *90*(1–2), 127–140. https://doi.org/10.1002/cite.201700129

Schorn, F., Breuer, J. L., Samsun, R. C., Schnorbus, T., Heuser, B., Peters, R., & Stolten, D. (2021). Methanol as a renewable energy carrier: An assessment of production and transportation costs for selected global locations. *Advances in Applied Energy*, *3*, 100050. https://doi.org/10.1016/j.adapen.2021.100050

Sherwin, E. D. (2021). Electrofuel synthesis from variable renewable electricity: An optimization-based techno-economic analysis. *Environmental Science & Technology*, *55*(11), 7583–7594. https://doi.org/10.1021/acs.est.0c07955

Sollai, S., Porcu, A., Tola, V., Ferrara, F., & Pettinau, A. (2023). Renewable methanol production from green hydrogen and captured CO_2: A techno-economic assessment. *Journal of CO2 Utilization*, *68*, 102345. https://doi.org/10.1016/j.jcou.2022.102345

Terlouw, T., Bauer, C., McKenna, R., & Mazzotti, M. (2022). Large-scale hydrogen production via water electrolysis: A techno-economic and environmental assessment. *Energy & Environmental Science*, *15*(9), 3583–3602. https://doi.org/10.1039/D2EE01023B

Terlouw, T., Rosa, L., Bauer, C., & McKenna, R. (2024). Future hydrogen economies imply environmental trade-offs and a supply-demand mismatch. *Nature Communications*, *15*(1), 7043. https://doi.org/10.1038/s41467-024-51251-7

Terlouw, T., Treyer, K., Bauer, C., & Mazzotti, M. (2021). Life cycle assessment of direct air carbon capture and storage with low-carbon energy sources. *Environmental Science & Technology*, *55*(16), 11397–11411. https://doi.org/10.1021/acs.est.1c03263

Tremel, A. (2018). *Electricity-based Fuels*. Springer International Publishing. https://doi.org/10.1007/978-3-319-72459-1

Van De Loosdrecht, J., Botes, F. G., Ciobica, I. M., Ferreira, A., Gibson, P., Moodley, D. J., Saib, A. M., Visagie, J. L., Weststrate, C. J., & Niemantsverdriet, J. W. (2013). Fischer–Tropsch synthesis: Catalysts and chemistry. In *Comprehensive inorganic chemistry II* (pp. 525–557). Elsevier. https://doi.org/10.1016/B978-0-08-097774-4.00729-4

Werker, J., Wulf, C., & Zapp, P. (2019). Working conditions in hydrogen production: A social life cycle assessment. *Journal of Industrial Ecology*, *23*(5), 1052–1061. https://doi.org/10.1111/jiec.12840

Wernet, G., Bauer, C., Steubing, B., Reinhard, J., Moreno-Ruiz, E., & Weidema, B. (2016). The ecoinvent database version 3 (part I): Overview and methodology. *The International Journal of Life Cycle Assessment*, *21*(9), 1218–1230. https://doi.org/10.1007/s11367-016-1087-8

Zhu, R., Wang, Z., He, Y., Zhu, Y., & Cen, K. (2022). LCA comparison analysis for two types of H_2 carriers: Methanol and ammonia. *International Journal of Energy Research*, *46*(9), 11818–11833. https://doi.org/10.1002/er.7947

SUPPORTING INFORMATION

Additional supporting information can be found online in the Supporting Information section at the end of this article.